

Evidence for the Triple-Gluon Vertex from Measurements of the QCD Colour Factors in Z Decay into 4 Jets

The ALEPH Collaboration¹

Abstract

A sample of 4148 four-jet events observed in the ALEPH-detector at LEP in 1989 and 1990 is used to test the underlying gauge group of strong interactions. A fit to the ratios of the “colour factors” C_F , N_C and T_F , which determine the differential cross sections, yields $N_C/C_F = 2.24 \pm 0.32_{stat} \pm 0.24_{syst}$ and $T_F/C_F = 0.58 \pm 0.17_{stat} \pm 0.23_{syst}$. This is in agreement with the values expected from QCD: $N_C/C_F = 2.25$ and $T_F/C_F = 0.375$. The non-zero value of N_C/C_F constitutes direct evidence for the existence of the triple-gluon coupling and excludes any Abelian gauge theory by more than five standard deviations.

(Submitted to Physics Letters B)

¹See the following pages for the list of authors.

The ALEPH Collaboration

D. Decamp, B. Deschizeaux, C. Goy, J.-P. Lees, M.-N. Minard

Laboratoire de Physique des Particules (LAPP), IN²P³-CNRS, 74019 Annecy-le-Vieux Cedex, France

R. Alemany, F. Ariztizabal, P. Comas, J.M. Crespo, M. Delfino, E. Fernandez, V. Gaitan, Ll. Garrido, Ll.M. Mir, A. Pacheco, A. Pascual

Institut de Fisica d'Altes Energies, Universitat Autònoma de Barcelona, 08193 Bellaterra (Barcelona), Spain⁸

D. Creanza, M. de Palma, A. Farilla, G. Iaselli, G. Maggi, M. Maggi, S. Natali, S. Nuzzo, M. Quattromini, A. Ranieri, G. Raso, F. Romano, F. Ruggieri, G. Selvaggi, L. Silvestris, P. Tempesta, G. Zito

INFN Sezione di Bari e Dipartimento di Fisica dell' Università, 70126 Bari, Italy

Y. Gao, H. Hu,²¹ D. Huang, X. Huang, J. Lin, J. Lou, C. Qiao,²¹ T. Wang, Y. Xie, D. Xu, R. Xu, J. Zhang, W. Zhao

Institute of High-Energy Physics, Academia Sinica, Beijing, The People's Republic of China⁹

W.B. Atwood,² L.A.T. Bauerdick, E. Blucher, G. Bonvicini, F. Bossi, J. Boudreau, T.H. Burnett,³ H. Drevermann, R.W. Forty, R. Hagelberg, S. Haywood, J. Hilgart, R. Jacobsen, B. Jost, M. Kasemann,²⁶ J. Knobloch, E. Lançon, I. Lehraus, T. Lohse, A. Lusiani, M. Martinez, P. Mato, T. Mattison, H. Meinhard, S. Menary,²⁷ T. Meyer, A. Minten, A. Miotto, R. Miquel, H.-G. Moser, J. Nash, P. Palazzi, J.A. Perlas, F. Ranjard, G. Redlinger, L. Rolandi,²⁸ A. Roth,³⁰ J. Rothberg,³ T. Ruan,^{21,33} M. Saich, D. Schlatter, M. Schmelling, F. Sefkow, W. Tejessy, H. Wachsmuth, W. Wiedenmann, T. Wildish, W. Witzeling, J. Wotschack

European Laboratory for Particle Physics (CERN), 1211 Geneva 23, Switzerland

Z. Ajaltouni, F. Badaud, M. Bardadin-Otwinowska, A.M. Bencheikh, R. El Fellous, A. Falvard, P. Gay, C. Guicheney, P. Henrard, J. Jousset, B. Michel, J.-C. Montret, D. Pallin, P. Perret, B. Pietrzyk, J. Proriot, F. Prulhière, G. Stimpfl

Laboratoire de Physique Corpusculaire, Université Blaise Pascal, IN²P³-CNRS, Clermont-Ferrand, 63177 Aubière, France

J.D. Hansen, J.R. Hansen, P.H. Hansen, R. Møllerud, B.S. Nilsson

Niels Bohr Institute, 2100 Copenhagen, Denmark¹⁰

I. Efthymiopoulos, A. Kyriakis, E. Simopoulou, A. Vayaki,¹ K. Zachariadou

Nuclear Research Center Demokritos (NRCD), Athens, Greece

J. Badier, A. Blondel, G. Bonneaud, J.C. Brient, G. Fouque, A. Gamess, J. Harvey, S. Orteu, A. Rosowsky, A. Rougé, M. Rumpf, R. Tanaka, H. Videau

Laboratoire de Physique Nucléaire et des Hautes Energies, Ecole Polytechnique, IN²P³-CNRS, 91128 Palaiseau Cedex, France

D.J. Candlin, M.I. Parsons, E. Veitch

Department of Physics, University of Edinburgh, Edinburgh EH9 3JZ, United Kingdom¹¹

L. Moneta, G. Parrini

Dipartimento di Fisica, Università di Firenze, INFN Sezione di Firenze, 50125 Firenze, Italy

M. Corden, C. Georgiopoulos, M. Ikeda, J. Lannutti, D. Levinthal,¹⁶ M. Mermikides[†], L. Sawyer, S. Wasserbaech
Supercomputer Computations Research Institute and Dept. of Physics, Florida State University, Tallahassee, FL 32306, USA^{13,14,15}

A. Antonelli, R. Baldini, G. Bencivenni, G. Bologna,⁵ P. Campana, G. Capon, F. Cerutti, V. Chiarella, B. D'Ettore-Piazzoli,³² G. Felici, P. Laurelli, G. Mannocchi,⁶ F. Murtas, G.P. Murtas, L. Passalacqua, M. Pepe-Altarelli, P. Picchi⁵

Laboratori Nazionali dell'INFN (LNF-INFN), 00044 Frascati, Italy

B. Altoon, O. Boyle, P. Colrain, I. ten Have, J.G. Lynch, W. Maitland, W.T. Morton, C. Raine, J.M. Scarr, K. Smith, A.S. Thompson, R.M. Turnbull

Department of Physics and Astronomy, University of Glasgow, Glasgow G12 8QQ, United Kingdom¹¹

B. Brandl, O. Braun, R. Geiges, C. Geweniger, P. Hanke, V. Hepp, E.E. Kluge, Y. Maumary, A. Putzer, B. Rensch, A. Stahl, K. Tittel, M. Wunsch

Institut für Hochenergiephysik, Universität Heidelberg, 6900 Heidelberg, Fed. Rep. of Germany¹⁷

A.T. Belk, R. Beuselinck, D.M. Binne, W. Cameron, M. Cattaneo, D.J. Colling, P.J. Dornan,¹ S. Dugeay, A.M. Greene, J.F. Hassard, N.M. Lieske, S.J. Patton, D.G. Payne, M.J. Phillips, J.K. Sedgbeer, G. Taylor, I.R. Tomalin, A.G. Wright

Department of Physics, Imperial College, London SW7 2BZ, United Kingdom¹¹

P. Girtler, D. Kuhn, G. Rudolph

Institut für Experimentalphysik, Universität Innsbruck, 6020 Innsbruck, Austria¹⁹

C.K. Bowdery, T.J. Brodbeck, A.J. Finch, F. Foster, G. Hughes, D. Jackson, N.R. Keemer, M. Nuttall, A. Patel, T. Sloan, S.W. Snow, E.P. Whelan

Department of Physics, University of Lancaster, Lancaster LA1 4YB, United Kingdom¹¹

T. Barczewski, K. Kleinknecht, J. Raab, B. Renk, S. Roehn, H.-G. Sander, H. Schmidt, F. Steeg, S.M. Walther, B. Wolf

Institut für Physik, Universität Mainz, 6500 Mainz, Fed. Rep. of Germany¹⁷

J.-J. Aubert, C. Benchouk, V. Bernard, A. Bonissent, J. Carr, P. Coyle, J. Drinkard, F. Etienne, S. Papalexiou, P. Payre, Z. Qian, D. Rousseau, P. Schwemling, M. Talby

Centre de Physique des Particules, Faculté des Sciences de Luminy, IN²P³-CNRS, 13288 Marseille, France

S. Adlung, H. Becker, W. Blum,¹ D. Brown, P. Cattaneo,²⁹ G. Cowan, B. Dehning, H. Dietl, F. Dydak,²⁵ M. Fernandez-Bosman, M. Frank, A.W. Halley, T. Hansl-Kozanecka,^{2,22} J. Lauber, G. Lütjens, G. Lutz, W. Männer, Y. Pan, R. Richter, H. Rotscheidt, J. Schröder, A.S. Schwarz, R. Settles, U. Stierlin, U. Stiegler, R. St. Denis, M. Takashima,⁴ J. Thomas,⁴ G. Wolf

Max-Planck-Institut für Physik und Astrophysik, Werner-Heisenberg-Institut für Physik, 8000 München, Fed. Rep. of Germany¹⁷

V. Bertin, J. Boucrot, O. Callot, X. Chen, A. Cordier, M. Davier, J.-F. Grivaz, Ph. Heusse, P. Janot, D.W. Kim,²⁰ F. Le Diberder, J. Lefrançois,¹ A.-M. Lutz, M.-H. Schune, J.-J. Veillet, I. Videau, Z. Zhang, F. Zomer

Laboratoire de l'Accélérateur Linéaire, Université de Paris-Sud, IN²P³-CNRS, 91405 Orsay Cedex, France

D. Abbaneo, S.R. Amendolia, G. Bagliesi, G. Batignani, L. Bosisio, U. Bottigli, C. Bradaschia, M. Carpinelli, M.A. Ciocci, R. Dell'Orso, I. Ferrante, F. Fidecaro,¹ L. Foà, E. Focardi, F. Forti, C. Gatto, A. Giassi, M.A. Giorgi, F. Ligabue, E.B. Mannelli, P.S. Marrocchesi, A. Messineo, F. Palla, G. Rizzo, G. Sanguinetti, J. Steinberger, R. Tenchini, G. Tonelli, G. Triggiani, C. Vannini, A. Venturi, P.G. Verdini, J. Walsh

Dipartimento di Fisica dell'Università, INFN Sezione di Pisa, e Scuola Normale Superiore, 56010 Pisa, Italy

J.M. Carter, M.G. Green, P.V. March, T. Medcalf, I.S. Quazi, J.A. Strong, L.R. West

Department of Physics, Royal Holloway & Bedford New College, University of London, Surrey TW20 OEX, United Kingdom¹¹

D.R. Botterill, R.W. Clift, T.R. Edgecock, M. Edwards, S.M. Fisher, T.J. Jones, P.R. Norton, D.P. Salmon, J.C. Thompson

Particle Physics Dept., Rutherford Appleton Laboratory, Chilton, Didcot, Oxon OX11 0QX, United Kingdom¹¹

B. Bloch-Devaux, P. Colas, W. Kozanecki,² M.C. Lemaire, E. Locci, S. Loucatos, E. Monnier, P. Perez, F. Perrier, J. Rander, J.-F. Renardy, A. Roussarie, J.-P. Schuller, J. Schwindling, D. Si Mohand, B. Vallage

*Service de Physique des Particules, DAPNIA, CE-Saclay, 91191 Gif-sur-Yvette Cedex, France*¹⁸

R.P. Johnson, A.M. Litke, J. Wear

Institute for Particle Physics, University of California at Santa Cruz, Santa Cruz, CA 95064, USA

J.G. Ashman, W. Babbage, C.N. Booth, C. Buttar, R.E. Carney, S. Cartwright, F. Combley, F. Hatfield, J. Martin, D. Parker, P. Reeves, L.F. Thompson

*Department of Physics, University of Sheffield, Sheffield S3 7RH, United Kingdom*¹¹

E. Barberio, S. Brandt, C. Grupen, L. Mirabito,³¹ U. Schäfer, H. Seywerd

*Fachbereich Physik, Universität Siegen, 5900 Siegen, Fed. Rep. of Germany*¹⁷

G. Ganis,³⁵ G. Giannini, B. Gobbo, F. Ragusa²⁴

Dipartimento di Fisica, Università di Trieste e INFN Sezione di Trieste, 34127 Trieste, Italy

L. Bellantoni, D. Cinabro,³⁴ J.S. Conway, D.F. Cowen,²³ Z. Feng, D.P.S. Ferguson, Y.S. Gao, J. Grahl, J.L. Harton, R.C. Jared,⁷ B.W. LeClaire, C. Lishka, Y.B. Pan, J.R. Pater, Y. Saadi, V. Sharma, M. Schmitt, Z.H. Shi, Y.H. Tang, A.M. Walsh, F.V. Weber, M.H. Whitney, Sau Lan Wu, X. Wu, G. Zoernig

*Department of Physics, University of Wisconsin, Madison, WI 53706, USA*¹²

[†]Deceased.

¹Now at CERN, PPE Division, 1211 Geneva 23, Switzerland.

²Permanent address: SLAC, Stanford, CA 94309, USA.

³Permanent address: University of Washington, Seattle, WA 98195, USA.

⁴Now at SSCL, Dallas, TX, U.S.A.

⁵Also Istituto di Fisica Generale, Università di Torino, Torino, Italy.

⁶Also Istituto di Cosmo-Geofisica del C.N.R., Torino, Italy.

⁷Permanent address: LBL, Berkeley, CA 94720, USA.

⁸Supported by CICYT, Spain.

⁹Supported by the National Science Foundation of China.

¹⁰Supported by the Danish Natural Science Research Council.

¹¹Supported by the UK Science and Engineering Research Council.

¹²Supported by the US Department of Energy, contract DE-AC02-76ER00881.

¹³Supported by the US Department of Energy, contract DE-FG05-87ER40319.

¹⁴Supported by the NSF, contract PHY-8451274.

¹⁵Supported by the US Department of Energy, contract DE-FC05-85ER250000.

¹⁶Supported by SLOAN fellowship, contract BR 2703.

¹⁷Supported by the Bundesministerium für Forschung und Technologie, Fed. Rep. of Germany.

¹⁸Supported by the Direction des Sciences de la Matière, C.E.A.

¹⁹Supported by Fonds zur Förderung der wissenschaftlichen Forschung, Austria.

²⁰Supported by the Korean Science and Engineering Foundation and Ministry of Education.

²¹Supported by the World Laboratory.

²²On leave of absence from MIT, Cambridge, MA 02139, USA.

²³Now at California Institute of Technology, Pasadena, CA 91125, USA.

²⁴Now at Dipartimento di Fisica, Università di Milano, Milano, Italy.

²⁵Also at CERN, PPE Division, 1211 Geneva 23, Switzerland.

²⁶Now at DESY, Hamburg, Germany.

²⁷Now at University of California at Santa Barbara, Santa Barbara, CA 93106, USA.

²⁸Also at Dipartimento di Fisica, Università di Trieste, Trieste, Italy.

²⁹Now at INFN, Pavia, Italy.

³⁰Now at Lufthansa, Hamburg, Germany.

³¹Now at Institut de Physique Nucléaire de Lyon, 69622 Villeurbanne, France.

³²Also at Università di Napoli, Dipartimento di Scienze Fisiche, Napoli, Italy.

³³On leave of absence from IHEP, Beijing, The People's Republic of China.

³⁴Now at Harvard University, Cambridge, MA 02138, U.S.A.

³⁵Supported by the Consorzio per lo Sviluppo dell'Area di Ricerca, Trieste, Italy.

1 Introduction

One consequence of the non-Abelian nature of QCD is the existence of a direct coupling between three gauge bosons, the so-called ‘‘Triple-Gluon Vertex’’ (TGV). Based on assumptions about the dominant parton-parton scattering processes the production of high- p_T jets in high-energy hadron collisions has been discussed as evidence for the existence of the TGV , see e.g. [1]. In e^+e^- annihilations the energy dependence of the three-jet cross section [2], where the TGV enters through loop corrections, constitutes another indirect evidence. Direct evidence at a fixed centre-of-mass energy can be obtained from the study of four-jet events where the TGV contributes already at tree level.

An analysis of four-jet events, based on test variables proposed by various authors [3, 4, 5, 6], has been used to study the TGV experimentally. These variables are sensitive either to the differences in the angular distributions of $q\bar{q}gg$ and $q\bar{q}q\bar{q}$ events or to the differences between contributions from double-bremsstrahlung diagrams and diagrams involving the triple-gluon coupling. Experimental results [7, 8, 9, 10] have been presented which show that the measured distributions of those test variables are consistent with QCD while a specific Abelian gluon model [3] could be excluded. This model is based on the three dimensional representation of the gauge group $U(1)$, denoted $U(1)_3$.

The DELPHI-collaboration has performed a simultaneous analysis [11] of two test variables with a first measurement of the colour factors of the theory of strong interactions, thereby not only eliminating one specific Abelian model but also restricting the range of alternative gauge groups.

This work generalizes this kind of analysis in a manner where one no longer refers to specific test variables but directly extracts the colour factors from the measured 5-fold differential four-jet cross section in a likelihood fit. This ensures that all selected four-jet events enter the analysis without any loss of information.

2 Theoretical Basis

Perturbative calculations of jet production in e^+e^- -annihilation processes to $\mathcal{O}(\alpha_s^2)$ have been performed by several authors [12, 13, 14, 15] for the case of massless partons. The results of reference [15] are the basis for the ‘‘matrix element’’ option in the JETSET [16] Monte-Carlo, in the following referred to as ‘‘Lund-ME’’ model. For any gauge group the differential cross sections derived from the diagrams shown in figure 1 factorize into kinematical and gauge group dependent terms:

- $q\bar{q}gg$ final states (figure 1 a-c):

$$\frac{1}{\sigma_0} d\sigma^{(4)} = \left(\frac{\alpha_s C_F}{\pi}\right)^2 \left[F_A(y_{ij}) + \left(1 - \frac{1}{2} \frac{N_C}{C_F}\right) F_B(y_{ij}) + \frac{N_C}{C_F} F_C(y_{ij}) \right] \quad (1)$$

- $q\bar{q}q\bar{q}$ final states (figure 1 d):

$$\frac{1}{\sigma_0} d\sigma^{(4)} = \left(\frac{\alpha_s C_F}{\pi}\right)^2 \left[\frac{T_F}{C_F} N_f F_D(y_{ij}) + \left(1 - \frac{1}{2} \frac{N_C}{C_F}\right) F_E(y_{ij}) \right], \quad (2)$$

where $y_{ij} = m_{ij}^2/s$ denotes the scaled invariant mass squared between any pair of partons i and j with $i, j = 1 \dots 4$ and N_f the number of active flavours. The analytical form of the kinematical functions $F_A \dots F_E$ can be extracted from Ref. [15]. The coefficients C_F, N_C and T_F are the colour

factors which for any representation of a gauge group describing the interaction can be calculated from its structure constants f^{abc} and its generators $(T^a)_{ij}$:

$$\sum_a (T^a T^{\dagger a})_{ij} = \delta_{ij} C_F \quad (3)$$

$$\sum_{a,b} f^{abc} f^{*abd} = \delta^{cd} N_C \quad (4)$$

$$Tr [T^a T^{\dagger b}] = \delta^{ab} T_F \quad (5)$$

In an intuitive way the colour factors can be identified with the fundamental couplings of the theory, as illustrated in figure 2. The colour factor C_F determines the strength of the coupling of a gluon to a quark or an antiquark, N_C describes the strength of the splitting of a gluon into two further gluons and T_F the strength of the splitting of a gluon into a quark-antiquark pair [17]. Therefore the ratio N_C/C_F is a direct measure of the relative strength of the TGV compared to the quark-gluon coupling.

For some common groups the colour factors are:

SU(N)	:	$N_C = N,$	$C_F = (N^2 - 1)/(2N),$	$T_F = 1/2$
QCD = SU(3)	:	$N_C = 3,$	$C_F = 4/3,$	$T_F = 1/2$
Abelian gluon model = U(1) ₃	:	$N_C = 0,$	$C_F = 1,$	$T_F = 3$
QED = U(1)	:	$N_C = 0,$	$C_F = 1,$	$T_F = 1$

Absorbing C_F into the normalisation of the cross sections (1) and (2), inter-jet correlations in four-jet events depend only on the ratios N_C/C_F and T_F/C_F . These ratios, which carry information about the gauge structure of the underlying theory, can be determined experimentally from a comparison of the differential four-jet cross section, measured as function of the scaled invariant masses squared y_{ij} , with the theoretical predictions.

3 Data Analysis

3.1 The ALEPH detector

The ALEPH detector, which provides tracking and calorimetric information over almost the full solid angle is described in ref. [18].

The charged particles are measured in two central tracking chambers. The inner tracking chamber (ITC) is a conventional drift chamber which provides up to 8 coordinates per track. The main chamber, a large time projection chamber (TPC) with radius of 1.8 m, yields up to 21 space points per track. Both chambers are located inside a superconducting solenoid. At the nominal magnetic field of 1.5 T a momentum resolution of $\delta p/p^2 = 0.0008/\text{GeV}$ is achieved by the combined system of TPC and ITC [19].

The electromagnetic calorimeter (ECAL) is a lead proportional tube sandwich with a total thickness corresponding to 22 radiation lengths with 45 read out layers. It is separated into three stacks corresponding to 4, 9 and 9 radiation lengths respectively. Anode wire signals are summed plane by plane for each module. Cathode pads of approximately $3 \times 3 \text{ cm}^2$ from consecutive planes are connected together to form towers pointing to the interaction region.

The hadron calorimeter (HCAL) is an iron streamer tube sandwich with 23 layers, segmented into 4800 projective towers.

In both calorimeters clusters are defined as groups of hit cells topologically connected. The energy of a cluster is the sum of the energies measured in its cells. Spurious clusters due to

electronic noise or malfunction are rejected by using the independent information provided by the wire readout of the ECAL or the streamer tube readout in the corresponding HCAL module. The accepted ECAL clusters can be identified as electromagnetic or hadronic clusters by virtue of the granularity of the calorimeter and taking advantage of the characteristic longitudinal and transverse profiles of electromagnetic and hadronic showers.

3.2 Event selection

The selected data consist of approximately 150000 hadronic events taken with the ALEPH detector at LEP in 1989 and 1990 at centre-of-mass energies around the Z mass.

All events are subjected to an energy flow analysis which makes use of the information coming from most of the ALEPH subdetectors. In particular, advantage is taken of the photon, electron and muon identification capabilities and of the redundancy of the energy measurements in the calorimeters. This energy flow algorithm provides information about charged and neutral, i.e. photon- and neutral hadron-like, particles. The principles of the energy flow algorithm are described in Ref.[20]. An energy resolution of 9% is achieved on the total energy at the Z mass.

To be used in the present analysis, charged particle tracks are required to be reconstructed with at least four space coordinates in the TPC and to originate from the beam-crossing point within 5 cm along the beam direction and 3 cm in the transverse direction. Furthermore, good tracks must have an angle of at least 20 degrees and a transverse momentum of $p_t \geq 200$ MeV/c with respect to the beam axis. Selected events are required to have at least 5 such charged tracks and a total charged energy in excess of 15 GeV.

To be considered in the subsequent analysis, the neutral clusters must have an energy of more than 300 MeV and their extrapolation to the beam-crossing point must form an angle of at least 20 degrees to the beam axis.

Finally, the total visible energy is required to be in excess of $0.5\sqrt{s}$ and the momentum imbalance along the beam direction of all accepted tracks and clusters to be smaller than $0.4\sqrt{s}$.

3.3 Reconstruction of four-jet events

The accepted events are fed into the PTCLUS [21] clustering algorithm which combines the good angular resolution of the LUCLUS [22] algorithm and the ability to reconstruct parton multiplicities of the JADE [23] algorithm. The algorithm takes the highest energy particle as the initiator of a first cluster and assigns to it all tracks with a relative transverse momentum below a certain threshold. The highest energy non-assigned track forms the initiator of another cluster which is treated the same way. The procedure is iterated until all tracks are assigned. The remaining clusters then are merged further using the JADE-scheme. In a final step those tracks which are not in the jet closest in angle are reassigned. The PTCLUS algorithm was used with the covariant E-scheme [24] merging, which is found to provide the best reconstruction of the lowest energy jet.

The clustering algorithm is required to produce exactly four clusters. In order to have a clean sample only those events are retained as four-jet events which for all pairs of clusters satisfy the cut

$$y_{ij} > y_{cut} = 0.03. \quad (6)$$

Here y_{ij} denotes the scaled invariant mass squared for clusters i and j calculated by

$$y_{ij} = \frac{2 E_i E_j \cdot (1 - \cos \theta_{ij})}{E_{vis}^2}, \quad (7)$$

where θ_{ij} is the angle between the jets, E_i and E_j are their energies and E_{vis} is the total visible energy of the event. The requirement $y_{cut} = 0.03$ ensures that the number of misidentified two- and three-parton events is small.

In addition the following cuts are applied to the four-jet sample: the angle to the beam axis for each jet is required to be above 20 degrees, the number of charged tracks or neutrals per jet at least two and the sum of the six scaled invariant masses squared above 0.95. This results in 4148 four-jet events passing all cuts.

Finally, in order to compare to the theoretical prediction, the y_{ij} are rescaled such that momentum conservation for four massless partons is fulfilled:

$$\sum_{i < j=1}^4 y_{ij} = 1 \quad . \quad (8)$$

3.4 Determination of the colour factors

The colour factors are determined from the data by a maximum likelihood fit of the second order theoretical prediction, i.e. by maximizing

$$\ln \mathcal{L} = \sum_i \ln \frac{\bar{\sigma}_i(N_C/C_F, T_F/C_F)}{\bar{\sigma}_{tot}(N_C/C_F, T_F/C_F)} \quad (9)$$

with respect to N_C/C_F and T_F/C_F . The sum runs over all selected four-jet events, $\bar{\sigma}_i$ denotes the folded four-jet cross section obtained by summing (1) and (2) over all permutations of parton-type assignments to the jets, thereby taking into account that no identification of parton type or quark flavour is done, and $\bar{\sigma}_{tot}$ is the corresponding total cross section. The ratio $\bar{\sigma}_i/\bar{\sigma}_{tot}$ then is the probability density for observing the event i for a given set of colour factors. The best fit values found for the data are $N_C/C_F = 2.76 \pm 0.25$ and $T_F/C_F = -0.12 \pm 0.17$.

Maximizing $\ln \mathcal{L}$ yields a measurement of N_C/C_F and T_F/C_F , but doesn't provide a criterium for the quality of the fit. One test of the fit quality can be performed by comparing the distribution of the individual log-likelihood values (equation (9)) to that obtained from Monte-Carlo data with well defined input colour factors. Comparing for example the data and the Lund-ME model the mean values of the distributions for the respective best fit values are $\langle \ln \mathcal{L} \rangle_{data} = 0.223 \pm 0.011$ and $\langle \ln \mathcal{L} \rangle_{ME} = 0.233 \pm 0.010$. The agreement indicates that the fit quality for the data is as good as expected. As a second test all one-dimensional projections on any y_{ij} -axis of the general 5-dimensional distribution were compared with the corresponding projections of the fitted cross sections. The fit quality was found to be good in all cases.

For the Lund-ME model the fitted colour factors are found to be $N_C/C_F = 2.75 \pm 0.20$ and $T_F/C_F = -0.31 \pm 0.14$ in agreement with the data. This is illustrated in figure 3, where the uncorrected distribution for the modified Nachtmann-Reiter angle [25] is compared both to the prediction of the Lund-ME model and the Abelian gluon model. Taking the statistical errors of the Monte-Carlo (not shown) into account one finds $\chi_{ME}^2/NdF = 9.8/9$ for the Lund-ME model and $\chi_{AM}^2/NdF = 38.8/9$ for the Abelian model. The sensitivity to the gauge structure of the theory is therefore already visible at the level of one-dimensional projections.

3.5 Correction procedure

Detector limitations and fragmentation effects, i.e. effects due to perturbative higher orders and hadronisation, lead to a shift of the measured colour factors with respect to the true values.

A correction for this effect is extracted from Monte-Carlo simulations based on a tuned version of the Lund-ME model. Even though the Lund-ME model in general does not describe the

structure of hadronic final states as well as the parton shower (PS) option of the Lund model [16], it is expected to be more suited for this analysis since it has the full second order matrix elements (1,2) used in the fit of the colour factors, while the PS option contains leading logarithms to all orders but is not complete in second order. 60000 four-parton final states are generated with y_{min} , the minimum scaled invariant mass squared of any two partons, set to $y_{min} = 0.01$. All events are passed through the full ALEPH detector simulation and the full reconstruction chain.

Reweighting the events generated with the Lund-ME model, thereby going to matrix elements with different colour factors, a two-dimensional correction function for N_C/C_F and for T_F/C_F is extracted. The results are parametrized in the following way:

$$\left(\frac{N_C}{C_F}\right)_c = c_0 + c_1 \left(\frac{N_C}{C_F}\right)_m + c_2 \left(\frac{T_F}{C_F}\right)_m + c_3 \left(\frac{N_C}{C_F}\right)_m^2 + c_4 \left(\frac{T_F}{C_F}\right)_m^2 + c_5 \left(\frac{N_C}{C_F}\right)_m \left(\frac{T_F}{C_F}\right)_m \quad (10)$$

$$\left(\frac{T_F}{C_F}\right)_c = d_0 + d_1 \left(\frac{N_C}{C_F}\right)_m + d_2 \left(\frac{T_F}{C_F}\right)_m + d_3 \left(\frac{N_C}{C_F}\right)_m^2 + d_4 \left(\frac{T_F}{C_F}\right)_m^2 + d_5 \left(\frac{N_C}{C_F}\right)_m \left(\frac{T_F}{C_F}\right)_m \quad (11)$$

The index m refers to the measured values and c to the corrected ones. The coefficients are given in Table 1. The uncertainty of this correction due to finite Monte-Carlo statistics is $\sigma_{MC}(N_C/C_F) = 0.11$ and $\sigma_{MC}(T_F/C_F) = 0.05$.

$c_0 =$	-1.193	$d_0 =$	0.618
$c_1 =$	1.121	$d_1 =$	0.052
$c_2 =$	-0.067	$d_2 =$	1.008
$c_3 =$	0.042	$d_3 =$	-0.007
$c_4 =$	0.027	$d_4 =$	0.008
$c_5 =$	-0.026	$d_5 =$	0.024

Table 1: *Coefficients of the correction functions (10) and (11)*

4 Systematic errors

The following sources of systematic uncertainties are discussed:

- Statistical uncertainty in the correction function
- Fragmentation uncertainties
- Experimental systematic errors
- Background from misidentified two- and three-parton events.

Table 2 summarizes the individual contributions. The statistical error of the correction function was already given in the previous section, the others are briefly discussed below. A more detailed description can be found in Ref. [26].

4.1 Fragmentation Uncertainties

The fragmentation uncertainties include uncertainties due to higher order corrections, mass and hadronization effects.

One way to estimate the importance of uncalculated higher order corrections is the variation of the renormalization scale μ . In second order perturbation theory the three-jet rate as well as

Source of uncertainty	σ_{N_C/C_F}	σ_{T_F/C_F}
statistical error of correction function	0.11	0.05
fragmentation uncertainty	0.08	0.20
experimental systematics	0.11	0.08
background from 2- and 3-parton events	0.10	0.08

Table 2: *Summary of systematic errors for the measurement of N_C/C_F and T_F/C_F*

the three-jet kinematics depend on the scale. For four-jet events only the rate is affected. Since this analysis only studies correlations within four-jet events, it is in principle not affected by scale uncertainties. Scale dependencies may however enter indirectly through the influence of the scale on the two- and three-parton cross sections, thereby affecting the number of background events which enter the four-jet sample. This background decreases for smaller scales. Since the analysis of the uncertainties due to background events uses a large scale ($\mu = M_Z$), any possible scale dependencies are covered by the error due to background.

In general higher order contributions not only change the rate of four-jet events but also the correlations between the jets. As a consequence the effective colour factors obtained from the comparison to pure second order perturbation theory are different from the true ones. This is corrected by the functions (10) and (11), which approximate all effects beyond $\mathcal{O}(\alpha_s^2)$ in the framework of the Lund-ME model, where both perturbative higher orders and hadronisation effects are modelled by the string fragmentation concept. The Lund-PS model does not contain the complete second order matrix element, but it includes leading logarithms in all orders of α_s . The four-parton level in the Lund-PS² model thus does not correspond exactly to the second order matrix element with QCD colour factors. Assuming that the leading-log contributions are dominant, the model is nevertheless suited to predict the shift in the colour factors due to higher order corrections. Since different missing higher order terms are simulated by the fragmentation process in the Lund-ME and the Lund-PS model, the shifts in the colour factors between the four-parton level and the hadron level are different. The difference in the shifts is therefore used as an estimate of the uncertainties due to higher order terms.

The partons in the matrix element model are on-shell, while the average off-shellness in the parton shower is approximately 2.5 GeV. Therefore the above estimate is assumed to include also uncertainties associated with the fact that the theory strictly applies only to massless partons.

The uncertainty related to the transition from the second order parton level to the hadron level defined above was determined using a dedicated high statistics Monte-Carlo production. The corresponding colour factors for both levels are given in table 3. For the parton shower model the shifts in the colour factors are found to be $\Delta_{PS}(N_C/C_F) = 0.96 \pm 0.04$ and $\Delta_{PS}(T_F/C_F) = -0.29 \pm 0.03$. The same shifts for the matrix element model are $\Delta_{ME}(N_C/C_F) = 0.99 \pm 0.04$ and $\Delta_{ME}(T_F/C_F) = -0.48 \pm 0.03$. Taking the differences of these shifts and adding the statistical errors in quadrature the contribution of higher order effects to the fragmentation uncertainties are obtained to be $\sigma_{ho}(N_C/C_F) = 0.06$ and $\sigma_{ho}(T_F/C_F) = 0.19$.

As an additional check the fragmentation parameters are varied. The ranges cover the values obtained from fitting the ALEPH data [27] and those parameters determined in reference [28] using small renormalization scales. Within the statistical uncertainties of the simulation no effect on the measured colour factors could be found. An upper limit is estimated to be

²The second-order parton level in the Lund-PS model was defined by the partonic configuration after the decay of the two partons with the highest virtual mass in the shower history.

$\sigma_{par}(N_C/C_F) = \sigma_{par}(T_F/C_F) = 0.05$ which is included in the total fragmentation uncertainty.

4.2 Experimental systematics

To estimate the systematic error due to the experimental procedure different combinations of merge- and clustering-algorithms, as described in [24], and different sets of cuts to define the four-jet sample were studied and the RMS-shift of the results taken as the systematic error. One finds $\sigma_{cuts}(N_C/C_F) = 0.07$, $\sigma_{cuts}(T_F/C_F) = 0.04$, $\sigma_{alg}(N_C/C_F) = 0.09$ and $\sigma_{alg}(T_F/C_F) = 0.07$. Adding both contributions in quadrature the experimental systematic errors are found to be $\sigma_{exp}(N_C/C_F) = 0.11$ and $\sigma_{exp}(T_F/C_F) = 0.08$.

4.3 Background from misidentified two- and three-parton events

To determine the systematic error due to background from misidentified two- and three-parton events an additional Monte-Carlo sample of 10000 events was studied with the same parameters as for the pure four-parton final states, but generating only two- and three-parton events. From these 5 events are misidentified as four-jet events, i.e. at 90% confidence level the misidentification probability is smaller than $p_{mis} = 9.3 \times 10^{-4}$. For the data sample this corresponds to an upper limit of 108 background events in the selected four-jet sample which bias the measured colour factors because of their different inter-jet correlations. The size of this bias is estimated by adding the log-likelihood function for the background events to the log-likelihood sum of the four-parton sample. The observed shift is taken to be the systematic error due to background. One obtains $\sigma_{bg}(N_C/C_F) = 0.10$ and $\sigma_{bg}(T_F/C_F) = 0.08$.

5 Results

After correction the ratios of the colour factors are obtained as $N_C/C_F = 2.24 \pm 0.32_{stat} \pm 0.24_{syst}$ and $T_F/C_F = 0.58 \pm 0.17_{stat} \pm 0.23_{syst}$. For the final errors all but the fragmentation errors and the uncertainties of the correction function were propagated through the correction. The correlation coefficient for the statistical errors is $\rho_{stat} = 0.065$. Taking the systematic errors given in table 2 to be uncorrelated yields a correlation coefficient $\rho = 0.043$ for all errors combined in quadrature.

The result is in agreement with QCD and also with the measurements $N_C/C_F = 2.55 \pm 0.71$ and $T_F/C_F = 0.02 \pm 0.48$ from the DELPHI analysis [11]. The Abelian gluon model is clearly excluded. Adding statistical and systematic errors in quadrature the ALEPH result rules out any alternative Abelian theory by more than five standard deviations. This is illustrated by figure 4 where this measurement including its 68% confidence level contour based on the combined errors is shown in a two-dimensional plot of T_F/C_F versus N_C/C_F . Also indicated are the expectations for all simple Lie-groups with the fundamental representation for the fermions and the expectation for the Abelian gluon model [29].

Table 3 summarizes the results of this analysis. The first three rows show how for QCD the colour factors measured by the likelihood fit shift when going from the second order parton level to the detector level after the full simulation. As the fourth row shows, the large shift between hadron level and full simulation can be understood mainly as a result of the selection cuts defining the four-jet sample, as described in sections 3.2 and 3.3. In fact, it is found that corrections based only on the selection cuts reproduce within 25% the corrections (10,11) extracted from the full simulation. This allows to compare the uncorrected results from the data to the predictions of different Monte-Carlo models obtained after applying the selection cuts defining the four-jet sample to the generator hadron level. Again the Lund-ME prediction is in agreement with the data while the Abelian gluon model is in clear disagreement. Interestingly, for this particular

Event sample	N_C/C_F	T_F/C_F
Lund-ME, parton level	2.32 ± 0.06	$+0.39 \pm 0.05$
Lund-ME, hadron level	3.31 ± 0.06	-0.09 ± 0.05
Lund-ME, full simulation	2.75 ± 0.20	-0.31 ± 0.14
Lund-ME, selection cuts	2.75 ± 0.20	-0.18 ± 0.15
Lund-PS, parton level	1.74 ± 0.06	-0.05 ± 0.05
Lund-PS, hadron level	2.70 ± 0.06	-0.34 ± 0.05
Lund-PS, selection cuts	2.13 ± 0.18	-0.42 ± 0.12
Abelian gluon model, selection cuts	1.33 ± 0.32	$+2.81 \pm 0.36$
DATA uncorrected	2.76 ± 0.25	-0.12 ± 0.17
DATA corrected	$2.24 \pm 0.32_{stat} \pm 0.24_{syst}$	$+0.58 \pm 0.17_{stat} \pm 0.23_{syst}$

Table 3: *Comparison of colour factors obtained from various Monte-Carlo models on parton, hadron and detector level, together with the uncorrected and the corrected fit results from the ALEPH data. The numbers for Lund-ME and Lund-PS for parton and hadron level are from a dedicted high statistics production.*

event sample the data favour the matrix element model over the parton shower model, as can be expected. This shows that the analysis is sensitive to the difference between the complete second order matrix elements and the leading-log approximation, which is clearly visible in the colour factors fitted at the parton level for both models (see table 3).

6 Conclusions

A new method to measure the gauge structure of the theory of strong interactions, using the differential four-jet cross sections, was applied to hadronic data taken with the ALEPH detector in 1989 and 1990. A sample of 4148 four-jet events was selected and analysed. The results for the ratios of colour factors $N_C/C_F = 2.24 \pm 0.40$ ($0.32_{stat}, 0.24_{syst}$) and $T_F/C_F = 0.58 \pm 0.29$ ($0.17_{stat}, 0.23_{syst}$) are in agreement with the QCD colour factors $(N_C/C_F)_{QCD} = 2.25$ and $(T_F/C_F)_{QCD} = 0.375$. The non-zero value of N_C/C_F is clear evidence for the existence of the triple-gluon vertex. Any Abelian theory is ruled out by more than five standard deviations.

Acknowledgements

We would like to thank Luis Alvarez-Gaume for useful discussions. We congratulate our colleagues of the Accelerator divisions for the good performance of LEP. We are grateful to the engineering and technical personnel at CERN and at the home institutes for their contributions to the success of ALEPH. Those of us not from member states wish to thank CERN for its hospitality.

References

- [1] A. Breakstone et al., *Phys. Lett.* **B 248** (1990) 220.
- [2] OPAL Collaboration, M.Z. Akrawy et al., *Phys. Lett.* **B235** (1990) 389.
- [3] J.G. Körner, G. Schierholz and J. Willrodt, *Nucl. Phys.* **B185** (1981) 365.
- [4] O. Nachtmann and A. Reiter, *Z. Phys.* **C16** (1982) 45.
- [5] M. Bengtsson and P.M. Zerwas, *Phys. Lett.* **B208** (1988) 306.
- [6] M. Bengtsson, *Z. Phys.* **C42** (1989) 75.
- [7] AMY Collaboration, I.H. Park et al., *Phys. Rev. Lett.* **62** (1989) 1713.
- [8] VENUS Collaboration, K. Abe et al., *Phys. Rev. Lett.* **66** (1991) 280.
- [9] L3 Collaboration, B. Adeva et al., *Phys. Lett.* **B248** (1990) 227.
- [10] OPAL Collaboration, M.Z. Akrawy et al., *Z. Phys.* **C49** (1991) 49.
- [11] DELPHI Collaboration, P. Abreu et al., *Phys. Lett.* **B255** (1991) 466.
- [12] A. Ali, J.G. Körner, Z. Kunszt, E. Pietarinen, G. Kramer, G. Schierholz and J. Willrodt, *Nucl. Phys.* **B167** (1980) 454.
- [13] K.J.F. Gaemers, J.A.M. Vermaseren, *Z. Phys.* **C7** (1980) 81.
- [14] D. Danckaert, P. De Causmaecker, R. Gastmans, W. Troost, T.T. Wu, *Phys. Lett.* **B114** (1982) 203.
- [15] R.K. Ellis, D.A. Ross and A.E. Terrano, *Nucl. Phys.* **B178** (1981) 421.
- [16] T. Sjöstrand, *Computer Phys. Comm.* **39** (1986) 347 ; T. Sjöstrand and M. Bengtsson, *Computer Phys. Comm.* **43** (1987) 367.
- [17] R. Cutler and D. Sivers, *Phys. Rev* **D16** (1977) 679.
- [18] ALEPH Collaboration, D. Decamp et al., *Nucl. Instr. and Meth.* **A294** (1990) 121.
- [19] W.B. Atwood et al., *Nucl. Instr. and Meth.* **A306** (1991) 446.
- [20] ALEPH Collaboration, D. Decamp et al., *Phys. Lett.* **B246** (1990) 306.
- [21] J.M. Scarr, I. ten Have, ALEPH Internal note 89-150, (1989).
- [22] T. Sjöstrand, *Computer Phys. Comm.* **28** (1983) 229.
- [23] JADE Collaboration, W. Bartel et al., *Z. Phys.* **C33** (1986) 23;
JADE Collaboration, S. Bethke et al., *Phys. Lett.* **B213** (1988) 235.
- [24] Z. Kunszt, P. Nason, G. Marchesini and B.R. Webber, “QCD” in “Z Physics at LEP 1”, *CERN Report*, CERN 89-08, Volume 1 (1989) 373.
- [25] G. Rudolph, “Physics at LEP”, Vol. 2, *CERN report* 86-02 (1986) 150.
- [26] F. Steeg, Ph.D. Thesis, University of Mainz, (1992).
- [27] ALEPH Collaboration, Decamp et al., “Properties of hadronic Z^0 decays and Test of QCD Generators”, *to be published*.
- [28] W. de Boer, H. Fürstenau and J. Köhne, *Z. Phys.* **C49** (1991) 141.

- [29] R.N.Cahn, “Semi-Simple Lie Algebras and Their Representations”, *Frontiers in Physics, Vol.59* Benjamin-Cummings (Menlo Park 1984);
W.G. McKay and J. Patera, “Tables of Dimensions, Indices and Branching Rules for Representations of Simple Lie Algebras”, *Lecture Notes in Pure and Applied Mathematics, Vol. 69*, Dekker (New York 1981).

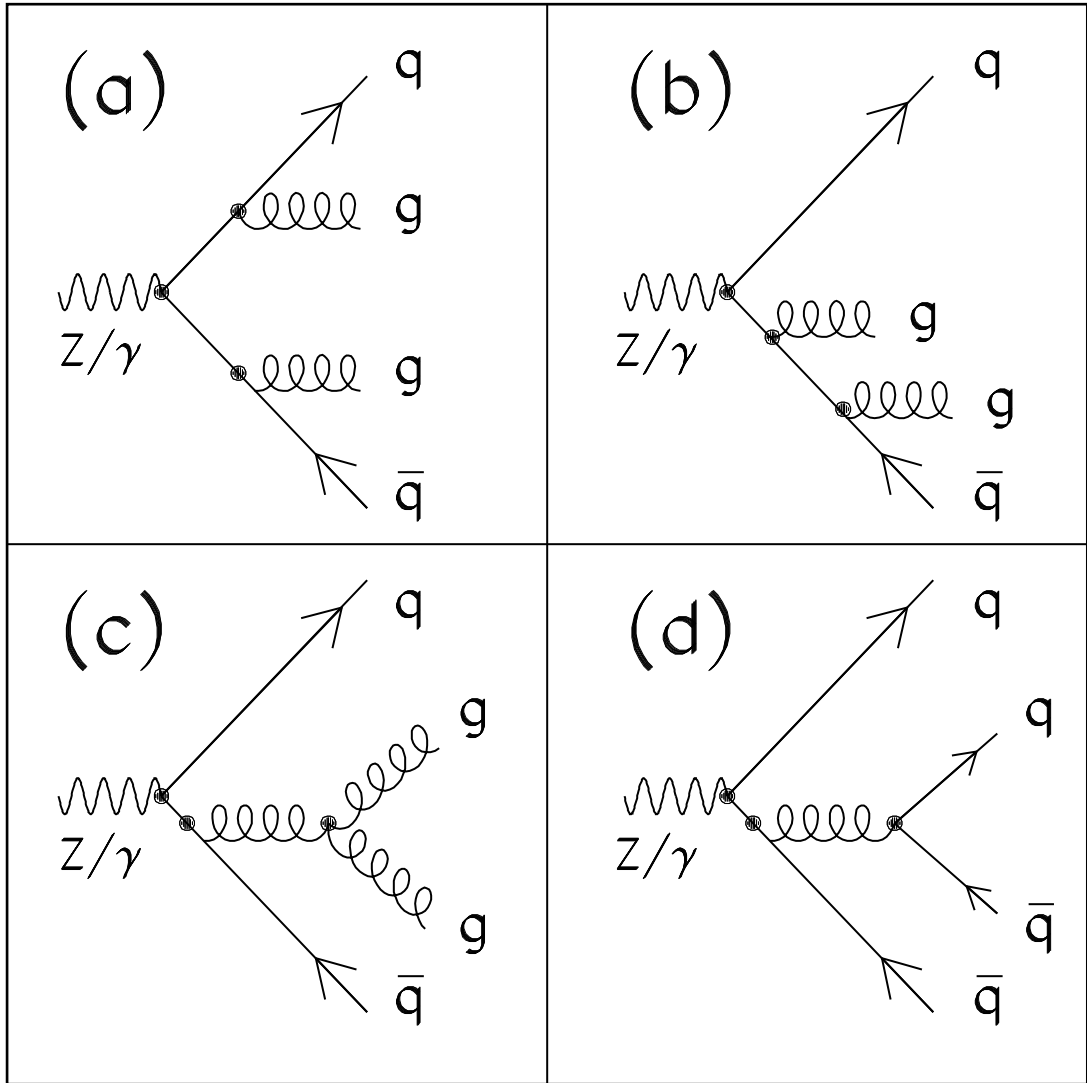


Figure 1: Classes of diagrams contributing to the four-jet cross section in second order QCD. The crossed amplitudes are not drawn.

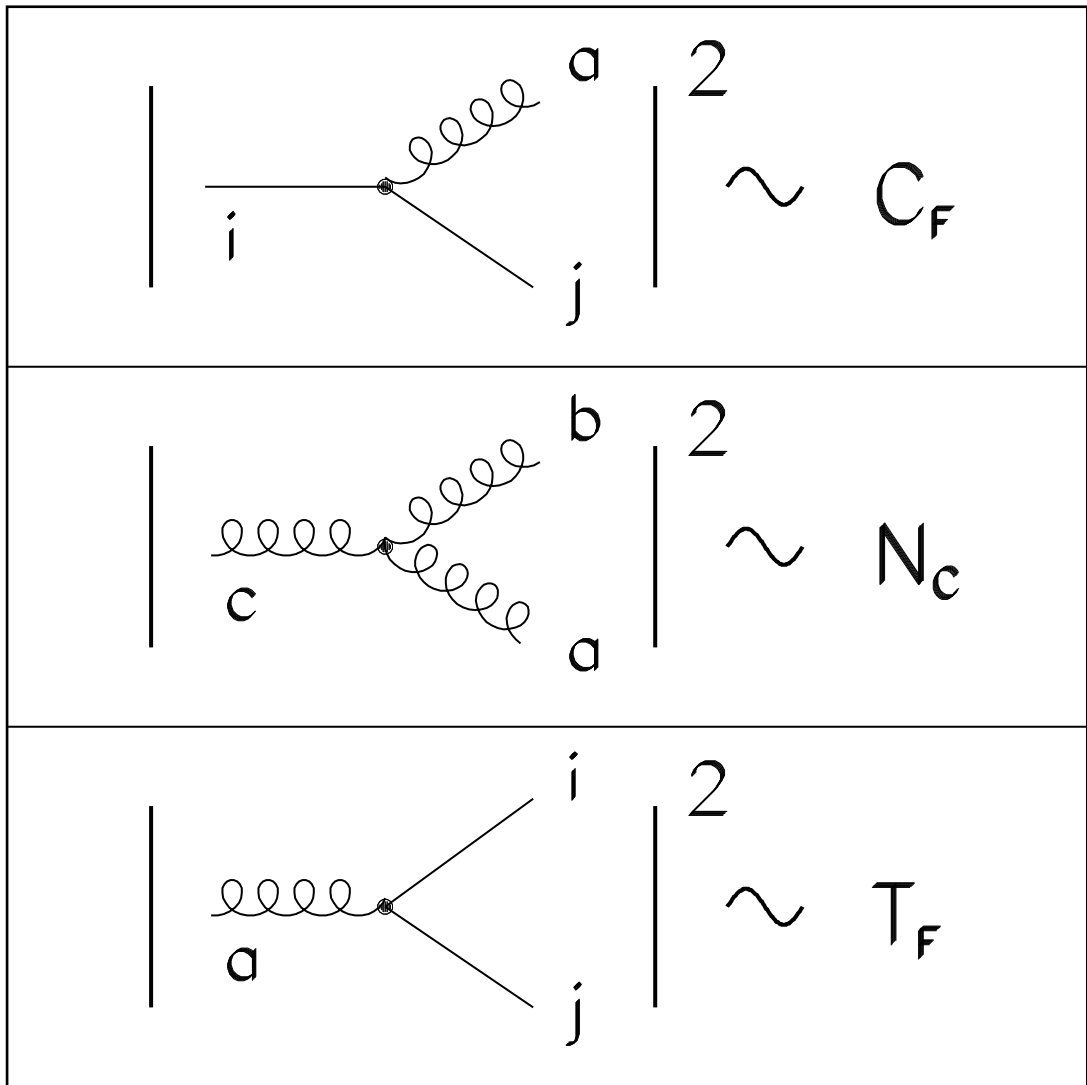


Figure 2: Definition of the colour factors in terms of fundamental couplings. The final state colour indices have to be summed.

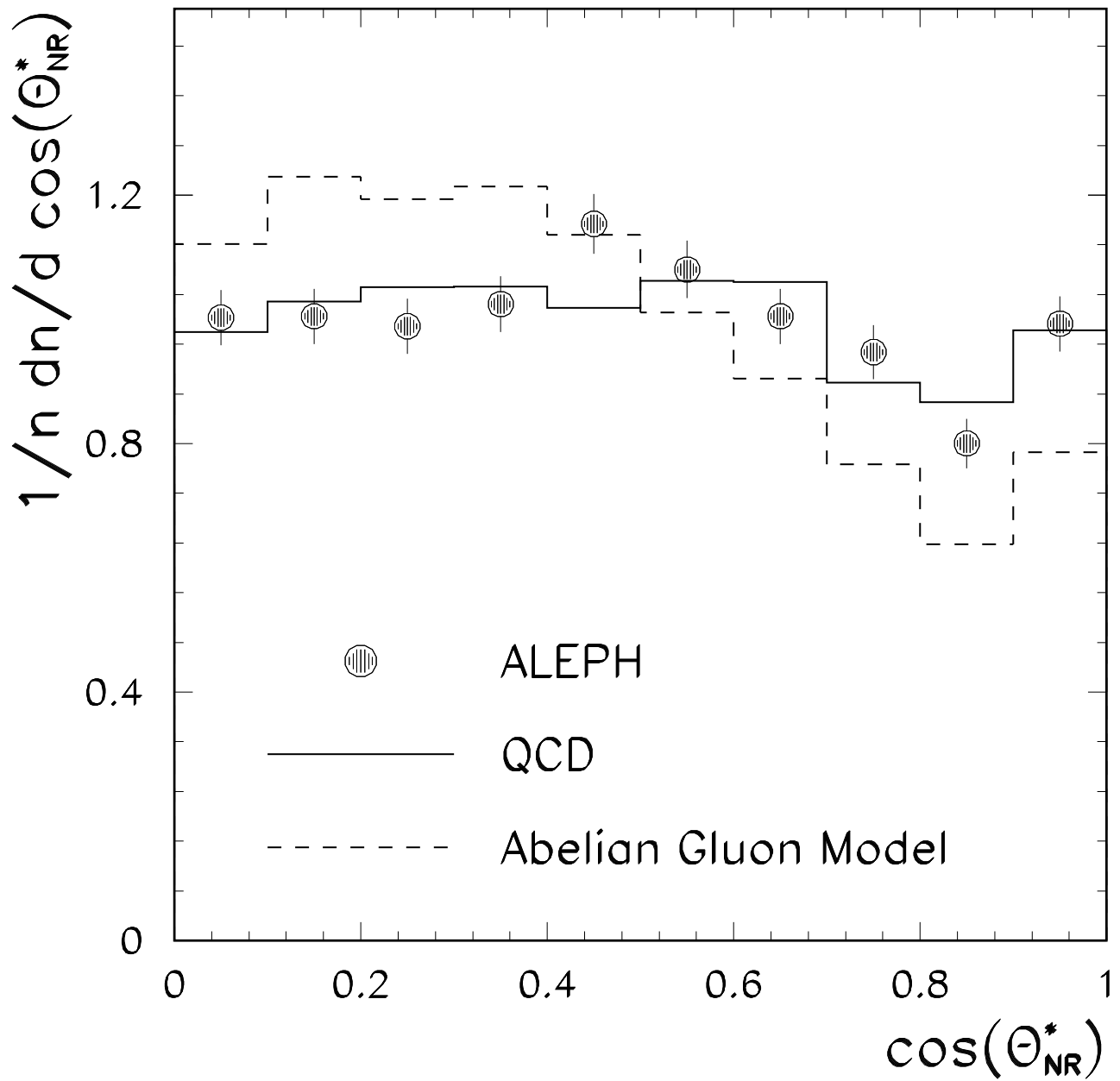


Figure 3: Uncorrected distribution of the modified Nachtmann-Reiter angle compared to QCD and the prediction from the Abelian gluon model.

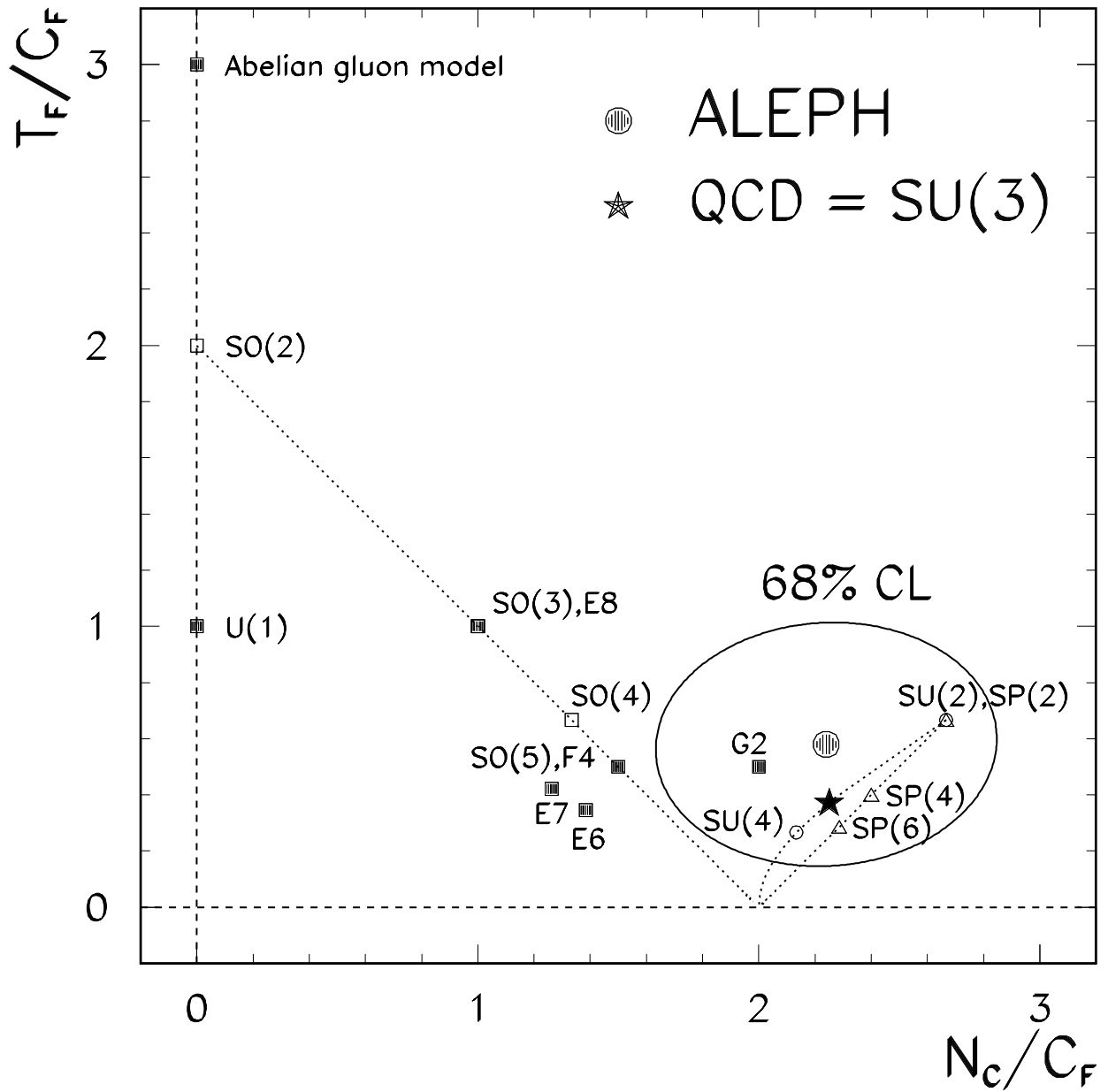


Figure 4: Measured ratios of colour factors compared to the prediction from different gauge theories. The dotted lines indicate the locations of the classical Lie-groups $SO(N)$, $SU(N)$ and $Sp(2N)$ for arbitrary N .